SKY DETECTION IN CSC-SEGMENTED COLOR IMAGES

Frank Schmitt and Lutz Priese
University of Koblenz-Landau, Koblenz, Germany*

Keywords: Sky detection, CSC.

Abstract: We present a novel algorithm for detection of sky areas in outdoor color images. In contrast to sky detectors in literature that detect only blue, cloudless sky we intend to detect all sorts of sky, i.e. blue, clouded and partially clouded sky. Our approach is based on the analysis of color, position, and shape properties of color homogeneous spatially connected regions detected by the CSC. An evaluation on a set of images acquired under different weather conditions proves the quality of the proposed system.

1 INTRODUCTION

For many applications in image processing accurate and fast detection of the sky is helpful. After the sky has been detected we can conclude on the content of the image and extract information about weather and illumination conditions during image acquisition. Knowledge about the sky also often helps to constrain the search domain for later, more complicated image recognition algorithms.

In images of urban regions the lower border of sky areas often equals the top border of buildings. Those borders can give first clues for pose estimation, i.e. the detection of position and orientation of the camera relative to the building. For this task it is important to find the sky reliable under all weather conditions, i.e., cloudless, partially clouded or overclouded. On the other hand, it is not important to find smaller isolated sky areas below such borders, e.g. under archways. The sky detection system introduced here is optimized for such an application scenario.

In the first steps of the algorithm, the input image is smoothed and segmented by the CSC, a region growing segmentation method introduced by Rehrmann and Priese (Rehrmann and Priese, 1998). The CSC partitions the image into spatially connected, color homogeneous regions, called segments. Each segment is analyzed individually regarding its mean color and a sky probability is attached. In a final step spatial information typical for urban scenes is added to the probability map and all segments are classified into sky and non-sky.

2 RELATED AND PREVIOUS WORK

Previous work on sky detection by other groups has the goal to detect the pure blue sky, thus, the image of the atmosphere. Clouds are by this definition explicitly not part of the sky and therefore not to be detected.

Luo and Etz (Luo and Etz, 2002) state that the color of the sky changes gradually from a dark blue in the zenith to a bright, sometimes almost white, blue near the horizon. They model the values in three color channels along straight lines from zenith to horizon as three one-dimensional functions and analyze these functions with regard to characteristic properties of the sky.

Gallagher et. al (Gallagher et al., 2004) first generate an initial sky probability map based on classification of color values. In a second stage they model the spatial variation of pixels initially classified as sky. They calculate for each color channel a two-dimensional polynomial that approximates the values of pixels with high sky probability. By comparison between values of pixels in the images and the corresponding values of the polynomial the final sky classification is generated.

Zafarifar and de With (Zafarifar and de With,

*This work was supported by the DFG under grant PR161/12-1 and PA 599/7-1

Schmitt F. and Priese L. (2009).
SKY DETECTION IN CSC-SEGMENTED COLOR IMAGES.
In *Proceedings of the Fourth International Conference on Computer Vision Theory and Applications*, pages 101-106
DOI: 10.5220/0001560601010106

2006) use sky detection in the context of image quality enhancement in video data. Their system generates a sky probability map based on texture, color values, gradients, and vertical position in the image. They achieve very good results, however, they only detect blue sky and therefore their system gives low sky probability in clouds.

However, in many parts of the world clouded sky is very common. Thus, systems which restrict themselves to blue sky detection are restricted in practicability. Our new system detects the total sky under all weather conditions.

First ideas of the presented approach – not including the following major improvements based on the analysis of segment's shape and gradients – have been presented in the German workshop "Farbworkshop 2008" (Schmitt and Priese, 2008).

3 CHARACTERISTICS OF SKY

In systems for the detection of a cloudless sky one may assume that the sky is free of large gradients but shows a continuous brightness gradient. As we regard clouds as part of the sky we can not make such an assumption. Our sky detector is thus based on different assumptions and observations of characteristics of the sky in color images in urban regions. We assume that the images to be analyzed have been acquired horizontally so that the sky is at the top of the image. Where this assumption does not apply one may employ algorithms for horizon estimation as introduced in (Ettinger et al., 2002) or (Fefilatyev et al., 2006).

Beside the position in the image, the color is the second characteristic property of the sky. The color can range from a pure white over different kinds of gray inside clouds to shades of blue of different saturation and brightness in cloudless regions. We further assume, that all segments belonging to the sky have a vertical connection to the upper border of the image, either directly or through other segments recognized as sky.

If one chooses, e.g., split-and-merge (Horowitz and Pavlidis, 1974) (SaM) as a segmentation technique and the sky disintegrates into several segments the borders between those segments show large straight lines. Those reflect the underlying quad-tree structure of the SaM algorithm. This will not happen with the CSC segmentation technique. The borders of two segments of the sky almost always show an irregular contour without straight lines. However, the border between sky and buildings is usually build from straight lines. This leads to further classification criteria.

4 THE ALGORITHM

4.1 Basic Concepts

Our algorithm is directly motivated by the observations of the previous paragraph.

In a first step we smooth the image and segment it into spatially connected, color homogeneous regions. In the next step we start at the top border of the image and search for segments whose mean color is suitable for sky.

However, an analysis of mean color and position is insufficient. Such a straight forward method also classifies white, gray, and blue objects outside the sky - but immediately below the horizon - as sky. To reduce the number of those false-positive classifications we have to add another step where the shape of possible sky segments is analyzed.

4.2 Pre-processing and Segmentation

The input image is first smoothed with one iteration of a 3×3 Kuwahara-filter (M. Kuwahara, K. Hachimura, S. Eiho, and M. Kinoshita, 1976). This non-linear filter sharpens borders and simultaneously smooths within homogeneous regions. The filtered image is segmented into spatially connected, color homogeneous regions with the CSC.

The CSC is a region growing segmentation method steered by a hierarchy of overlapping islands. If two overlapping partial segments are similar enough they are merged into a new segment. Else the common sub-region is split between them. As the decision whether to split or to merge two regions is not only based on a common border but a common sub-region, the results are more stable than in conventional region growing methods. The structure of the island hierarchy makes the CSC inherently parallel. Also, there is no need for spreading seed points in the image whose position influences the outcome of the segmentation in conventional region growing methods.

It is important to choose the parameters of the CSC such that an over-segmentation (areas belonging together are split into several segments) is more likely than an under-segmentation (areas not belonging together are merged into one segment) as an additional classification of the found segments has to been done anyway.

The CSC segmentation can be applied either in HSV color space based on color similarity tables (Rehrmann, 1994) or in L*a*b* color space where similarity between two shades of color is calculated using the Euclidean distance. For the experiments in

this paper we have chosen the L*a*b* color space with a threshold of 12. The result of the CSC is a label image where the value at every pixel is set to the label of the segment it belongs to.

4.3 Characteristics of Segments

Let a segment S be represented as a set of spatially connected pixels. The upper border $b_u(S)$ consists of all coordinates (x,y) such that the pixel at (x,y) is inside S and the pixel at (x,i) is outside S for all $i \in \mathbb{N}$ with $i < y$. (As customary in computer vision, we use positive coordinates (x,y) where $(0,0)$ denotes the left upper corner of the image.)

The *color* of S is the mean color of all pixels belonging to S. As segments are color homogeneous, the problem that averaging may create false colors does not occur.

The *mean vertical gradient* of S is a measure describing the brightness gradient at the common border between S and its upper neighbor segments. It is calculated as the average brightness difference between pixels at $b_u(S)$ and their direct upper neighbor pixels. If no upper neighbors exist the mean vertical gradient is set to 0. A low mean vertical gradient is a strong clue for a segment border generated during splitting of a color gradient into several segments. Such borders are normally more or less arbitrary and typical for a segmentation within the sky.

The *mean bounded second derivative* of $b_u(S)$ is a measure which describes whether the top border of S is build of straight lines or rather formed irregularly. It is calculated as follows:

Let x_{min} be the x-coordinate of the leftmost and x_{max} of the rightmost pixel in S. For each $i \in \mathbb{N}$ in $[x_{min}, x_{max}]$ exists exactly one coordinate with x-component i in $b_u(S)$. We can therefore regard $b_u(S)$ as a function of x where $b_u(S,x) := y$ if $(x,y) \in b_u(S)$ and undefined else. The function

$$\delta^2(S,x) := b_u(S,x-1) - 2 \cdot b_u(S,x) + b_u(S,x+1)$$

is the discrete second derivative of b_u for segment S at position x.

$|\delta^2(S,x)|$ is low at straight border segments and high at irregularly formed areas. Thus, an obvious approach would be to average $|\delta^2(S,x)|$ over the width of S in order to get a measure for the straightness of S. However, this approach leads to the problem that within a polygon, that consists of few connected straight lines, the corner points may contribute too high values. We therefore use bounded values as follows: Let $m(S,x) := 1$ for $|\delta^2(S,x)| \geq 1$ and $m(S,x) := 0$ elsewhere. The *mean bounded second derivative* of the top border of S is calculated as

$$\frac{\sum_{(x,y) \in b_u(S)} m(S,x)}{\sum_{(x,y) \in b_u(S)} 1}$$

4.4 Color Analysis

A classification of segments as sky solely by their color is obviously impossible. There are usually several objects (or reflections) in an image that do not belong to the sky but have a color which could also occur in the sky. Thus, in this phase we only determine whether the mean color of a segment may occur also in the sky. For such a task it will not help to train a classifier with many examples of sky and non-sky segments. The result will not be disjunctive as all colors which can occur in the sky can occur in other image regions as well. Instead, we were able to determine by manual analysis of sample images a simple and rather compact subspace of the HSV color space which includes all colors occurring in sky.

Our experiments have shown that it suffices to call a HSV value hsv *sky colored* if it meets at least one of the following conditions:

- hsv.saturation $<$ 13 and hsv.value $>$ 216
- hsv.saturation $<$ 25 and hsv.value $>$ 204 and hsv.hue $>$ 190 and hsv.hue $<$ 250
- hsv.saturation $<$ 128 and hsv.value $>$ 153 and hsv.hue $>$ 200 and hsv.hue $<$ 230
- hsv.value $>$ 88 and hsv.hue $>$ 210 and hsv.hue $<$ 220

The listed hue values are to some degree dependent on the cameras used.

4.5 Analysis of Position and Shape

Let L_s and L_c be two (initially empty) lists of segments already classified as sky (L_s) or as candidates (L_c) for sky. Segments whose mean color is sky colored and for which the condition holds that at least half of their top border touches the top border of the image are added to L_s. All segments touching the lower border of at least one of the segments in L_s are added to a L_c. For each segment S in L_c we check three criteria:

1. the color of S is sky colored,
2. at least two thirds of the top border of S touches either the top border of the image or segments in L_s,
3. at least one of the following conditions is satisfied:
   (a) the area of S contains less than 500 pixel (we skip shape analysis for such small segments)

(b) the mean vertical gradient of S is below 25

(c) the mean bounded second derivative of $b_u(S)$ is bigger than 0.3.

If all three conditions are satisfied S is classified as sky and the lists L_s, L_c are updated. Otherwise, S is removed from L_c. The algorithm terminates when the candidate list is empty.

At this stage, all segments which belong to sky and have a connection to the top border of the image (either a direct connection or through other sky segments) should have been classified as sky. However, in rare cases it may occur that, e.g., a cloud matches conditions 1 and 2 but not condition 3 and, thus, has been falsely classified as non-sky. Such cases are detected and fixed in a post-processing step where all non-sky segments which satisfy conditions 1 and 2 and which are completely surrounded by sky are classified as sky as well.

5 EVALUATION

For an evaluation 179 images of the campus of our university have been acquired under different weather conditions. Some examples are shown in appendix A. To get a ground truth (GT) we have manually annotated the sky to copies of those images. Our evaluation compares the detected sky with this ground truth sky with two measures: The *coverability rate* (CR) measures how much of the true sky is detected by the algorithm. The *error rate* (ER) measures how much of the area detected as sky is not part of the true sky. Let S denote the detected sky and GT the ground truth sky. Then both measures are defined as

$$CR(S,GT) := \frac{|S \cap GT|}{|GT|}, ER(S,GT) := \frac{|S - GT|}{|S|}$$

Graphic 1 visualizes our evaluation results. On the x-axis the error rates are shown, on the y-axis the coverability rates. The length of a line in z-direction at position (x,y) tells in how many cases error rate x and coverabiliy rate y was achieved. Graphics 2 and 3 show the distributions of CR and ER alone.

In 80% of all images, CR is above 0.9 and ER is below 0.1. In 75% of all images, CR is above 0.95 and ER is below 0.05. Those results clearly show the quality of the proposed algorithm. The cases where the error rate is very high correspond in the majority of cases to images that do not contain any sky at all. As soon as our algorithm classifies at least one pixel as sky in those images the error rate becomes 1.0.

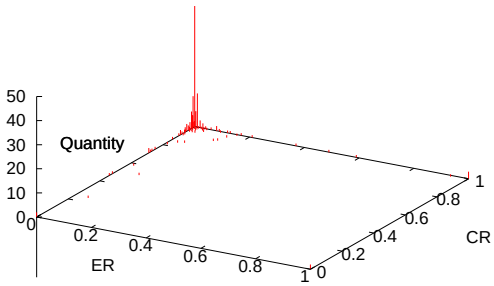

Figure 1: Distribution of CR and ER.

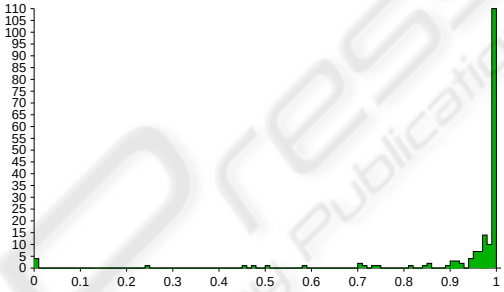

Figure 2: Distribution of CR.

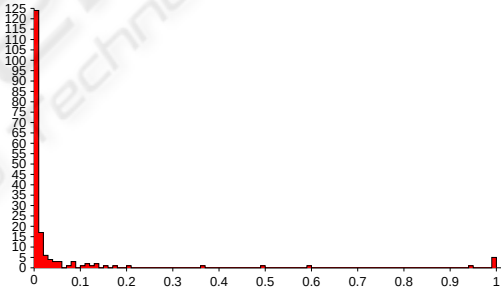

Figure 3: Distribution of ER.

6 SUMMARY AND OUTLOOK

We have presented a fast and robust system for detection of sky in camera images. In contrast to known systems, our algorithm is able to not only detect blue but also clouded sky. The presented algorithm is fast and an quantitative evaluation on a set of 179 images shows its robustness.

We intend to further improve our sky detector and will try to automatically detect and split segments which include both sky and non-sky, see Figure 7 as an example. Also the detection of images in urban scenes without any sky at all could be improved.

REFERENCES

Ettinger, S. M., Nechyba, M. C., Ifju, P. G., and Waszak, M. (2002). Towards flight autonomy: Vision-based horizon detection for micro air vehicles. In *Florida Conference on Recent Advances in Robotics 2002*.

Fefilatyev, S., Smarodzinava, V., Hall, L. O., and Goldgof, D. B. (2006). Horizon detection using machine learning techniques. In *ICMLA '06: Proceedings of the 5th International Conference on Machine Learning and Applications*, pages 17–21, Washington, DC, USA. IEEE Computer Society.

Gallagher, A. C., Luo, J., and Hao, W. (2004). Improved blue sky detection using polynomial model fit. In *Image Processing, 2004. ICIP '04. 2004 International Conference on*, volume 4, pages 2367–2370.

Horowitz, S. and Pavlidis, T. (1974). Picture segmentation by a directed split-and-merge procedure. In *Proceedings of the Second International Joint Conference on Pattern Recognition*, pages 424–433.

Luo, J. and Etz, S. P. (2002). A physical model-based approach to detecting sky in photographicimages. *IEEE Transactions on Image Processing*, 11(3):201–212.

M. Kuwahara, K. Hachimura, S. Eiho, and M. Kinoshita (1976). Processing of ri-angiocardiographic images. In Preston, K. and Onoe, M., editors, *Digital Processing of Biomedical Images*, pages 187–202.

Rehrmann, V. (1994). *Stabile, echtzeitfähige Farbbilddauswertung*. PhD thesis, Universität Koblenz-Landau, Fölbach Verlag, Koblenz.

Rehrmann, V. and Priese, L. (1998). Fast and robust segmentation of natural color scenes. In Chin, R. T. and Pong, T.-C., editors, *3rd Asian Conference on Computer Vision (ACCV'98)*, number 1351 in LNCS, pages 598–606. Springer Verlag.

Schmitt, F. and Priese, L. (2008). Himmelsdetektion in CSC-segmentierten Farbbildern. In *Farbworkshop 2008, Aachen*.

Zafarifar, B. and de With, P. H. N. (2006). Blue sky detection for picture quality enhancement. In *Advanced Concepts for Intelligent Vision Systems*, volume 4179/2006 of *Lecture Notes in Computer Science*, pages 522–532. Springer Berlin / Heidelberg.

APPENDIX

Sample Images

In the following images 4 to 6 the input image of our algorithm is shown on the left and the result of classification on the right. White represents segments classified as sky, gray represents segments which are sky colored but not classified as sky, black represents segments which are not sky colored.

The following picture 7 shows an example where the algorithm fails to correctly identify the sky. The segment encircled in red was falsely classified as sky as even in the CSC-segmentation phase the white front was melted into a larger sky segment.

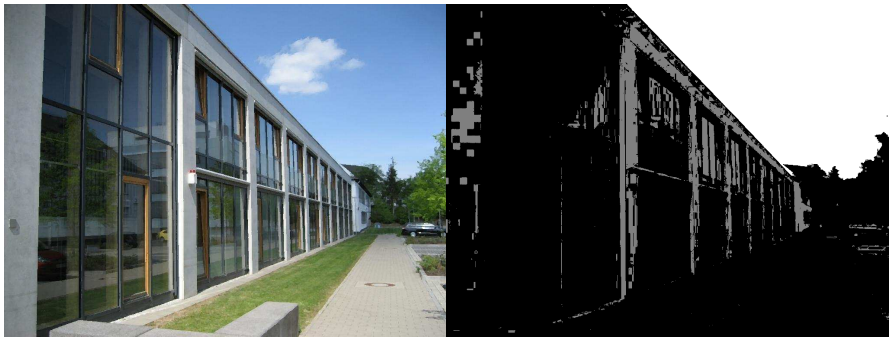

Figure 4: Photo taken at sunshine with fair-weather cloud.

Figure 5: Photo taken in rainy weather.

Figure 6: Sky colored segments in a building front which aren't classified as sky due to shape analysis.

Figure 7: Erroneous CSC segmentation: A white building front merges into one segment with the heavily clouded sky.